JOURNAL OF CATALYSIS 1, 416–431 (1962)

Field-Emission Study of Composite Adsorption Layers on Tungsten and Platinum

W. J. M. ROOTSAERT, L. L. VAN REIJEN, AND W. M. H. SACHTLER

From the Koninklijke/Shell-Laboratorium, Amsterdam
(Shell Internationale Research Maatschappij N.V.)

Received May 11, 1962

Physical adsorption of xenon on tungsten and chemisorption of hydrogen, carbon monoxide, and formic acid on both tungsten and platinum have been investigated in the field-emission microscope. Surface potentials are determined from Fowler-Nordheim plots; heats of adsorption of individual complexes on individual crystal faces are derived from measured desorption rates.

Four chemisorbed complexes are identified for hydrogen and also for carbon monoxide on tungsten. The adsorption of xenon and the majority of the chemisorbed complexes show a distinct topographic dependence; i.e. their heats of adsorption depend on the crystal face. These differences are more pronounced for the b.c.c. than for the f.c.c. lattice. The bond strengths on individual sites correlate with the number of surface atoms contacted simultaneously and with their degree of unsaturation. At low over-all coverage the adsorbate is concentrated on the faces with highest heat of adsorption, these faces becoming populated mainly by surface migration from less attractive faces. Only at very low temperature, where surface migration is severely restricted, does a uniform distribution of the adsorbate over the crystal faces result.

While the results confirm an important *a priori* heterogeneity of adsorption, they do not exclude "induced" effects, since certain complexes are only observed on faces which are precovered with other complexes of the same adsorbate.

I. Introduction

Numerous investigations on chemisorption by metals have led to speculations about the molecular description of this phenomenon. Some observations seem to indicate that all adsorption centers on a given metal have almost equal properties; other data suggest that adsorbing surfaces are composed of various types of sites of greatly different quality. Depending on the model chosen, the observed decrease of the heat of adsorption with increasing coverage is attributed to either an "induced" or to an *a priori* heterogeneity of the adsorbing sites.

New interest in this controversial problem arose from the discovery of "composite" adsorption layers on metals. In a composite layer different types of adsorption complexes are simultaneously present. This is demonstrated most conspicuously when, during the adsorption of a pure gas, complexes of opposite polarity appear in succession.

The oldest example on record seems to be hydrogen on platinum; in 1929 Suhrmann (*1*) concluded from his photoelectric measurements that two sorts of hydrogen can be present on the surface of a platinum foil. In 1950 Mignolet (*2*) reported that the work function of transition-metal films passed through a maximum when the surfaces were gradually covered with hydrogen. Others (*3, 4, 5*) found that the electric resistance of nickel films when plotted versus the hydrogen coverage θ, shows two

extrema, which indicates the presence of three discernible complexes. Thermodynamic properties of individual complexes in composite layers were investigated by Ehrlich (*6, 7, 8*), Hickmott (*9*), and Becker (*10, 11*), who were able to determine the individual θ values, the corresponding heats, and surface potentials by using the flash filament technique and field-emission microscopy.

The occurrence of composite layers proves that molecules can react in various ways with an adsorbing surface. The interpretation of the majority of data is, however, ambiguous as it still depends on the assumptions made about the nature of the adsorbing sites.

If an "*a priori* heterogeneity" of sites is assumed, one can imagine that heat of adsorption and bond type will be different on different types of sites (e.g. crystal faces). While the surface coverage is gradually increased different bond types will be observed successively, provided that the adsorbate has sufficient mobility for establishing equilibrium distribution on the surface.

If, on the other hand, identical adsorption sites are assumed, one can argue that every molecule, once it has been adsorbed, becomes part of the solid and consequently changes the physical properties of the latter, including the set of potential energy curves offered to the next impinging molecule. At a critical coverage the potential energy minimum, characterizing the bond type used, might have become so much flattened by this induced effect, that some other bond type starts to compete.

In the present paper we describe a study of the physical adsorption of xenon on tungsten and the chemisorption of hydrogen, carbon monoxide, and formic acid on tungsten and platinum. Composite adsorption layers have been carefully analyzed by means of field-emission microscopy in order to decide to what extent the bond type of adsorption is governed by *a priori* heterogeneity and to what extent "induced" effects come into play. Pursuing ideas published previously (*12*) correlations have been sought between the properties of individual adsorption complexes and the properties of the adsorbing sites, such as their shape, their size, and the degree of unsaturation of adjacent metal atoms.

II. Experimental

The most appropriate method for studying the phenomena mentioned above appears to be field emission, for the following reasons:

1. The small size of the cathode tip causes its shape to be nearly hemispherical in thermodynamic equilibrium. Even rough faces are stable and can readily be studied.
2. The high magnification allows of following processes at nearly atomic dimensions.
3. A controlled perfect cleaning of the adsorbing single crystal is possible.
4. Surface potentials of adsorbates can be measured on individual crystal faces.
5. Activation energies for desorption can be determined for individual crystal planes.
6. Migrations of adsorbates over the surface can be observed directly.

The method provides comparatively little information on crystal faces of very high work function, which hardly contribute to the electron emission from the tip surface. For the present study, this is not felt as a serious restriction, since the faces of high work function are smooth and therefore of comparatively little topographic interest.

The principle of field-emission microscopy and its experimental setup have been described in the literature (*13, 14*). In the present experiments, the pressure was kept below 10^{-10} mm Hg prior to gas adsorption. To avoid electron–molecule collisions during ad- or desorption experiments, the voltage was switched off as soon as the pressure exceeded 10^{-7} mm Hg. All current–voltage curves were reproducible when care was taken that the product of the emission current (in amperes) and the pressure (in mm Hg) never exceeded a value of 10^{-14}. Results of our earlier experiments (*12*), where this precaution had not been taken are, in part, invalidated by the present results.

Gases were usually admitted through a bakable Alpert gauge. This method is, however, not applicable for HCOOH, which decomposes in contact with metal surfaces; this substance was therefore brought into the cell by repeated high-vacuum sublimation in glass vessels. The electrolytically etched tungsten tips were cleaned thermally above 2500°C, the platinum tips were first exposed to oxygen in order to oxidize carbon impurities, then reduced by hydrogen and degassed thermally until all impurities had been removed.

The work functions were derived from the current–voltage characteristics which obeyed the Fowler-Nordheim equation

$$i = AV^2 \exp(-B\Phi^{3/2}/V) \qquad (1)$$

where: i = emission current; V = applied voltage; Φ = work function; and A,B = constants.

The constant A was found to be different for gas-covered and clean tips. For rapidly changing surface states, where no complete Fowler-Nordheim plots could be recorded, Φ was derived from the emission current i at constant voltage, by inserting in Eq. (1) a value of A obtained by interpolation from neighboring states, where complete Fowler-Nordheim plots had been taken.

The surface potential, characterizing any adsorption state is given by the definition

$$v = \Phi_0 - \Phi$$

A positive value of v indicates a positive charge on the adsorbate with respect to the adsorbing metal surface.

Activation energies for desorption E_{des} were derived from observed desorption rates. If τ is the half-life period (observed visually on the screen) of an adsorbed complex at temperature T, it follows from the theory of absolute reaction rates, that in fair approximation

$$E_{des} = RT \ln (kT/h)\,\tau$$

where h and k have their usual meaning. For the application of this equation it is decisive that readsorption be suppressed in the desorption measurements. The pressure was therefore kept at 10^{-9} mm Hg in these experiments. As adsorption is little or not activated in the cases studied, the activation energy for desorption is nearly equal to the heat of adsorption. The slight difference between E_{des} and ΔH_{ads} can be neglected *a fortiori* if only differences between heats of adsorption on various crystal faces are to be discussed.

III. Results

A. Physical Adsorption of Xenon on Tungsten

This system has thoroughly been studied by Ehrlich and Hudda (*6*) who used the same method. Our data agree with their results in every respect as is illustrated, e.g. by a comparison of their emission patterns with those given in Fig. 1. At 78°K and 10^{-8} mm Hg, adsorption of xenon causes a decrease in the work function of tungsten of 1.4 volts [Ehrlich and Hudda (*6*); 1.4 volts; Mignolet (*15*); 1.14 volts; Hermann (*16*): 0.64 volt*]. For the heats of adsorption we find:

$$\Delta H_{(411)} = 7.5 \text{ kcal/g atom}$$
$$\Delta H_{(111)} = 5.0 \text{ kcal/g atom}$$

The bright arcs between the (211)** and the (411) faces, visible in Fig. 1, expand into the (411) faces while adsorption proceeds. No arcs are observed during desorption.

B. Chemisorption of Hydrogen on Tungsten

Of the numerous experiments done with this system, three sets appear particularly instructive:

(a) A bare tungsten tip is exposed to hydrogen at 300°K and a pressure of 10^{-7} mm Hg. While the pressure is kept constant, the temperature is lowered to 78°K and then repeatedly varied slowly between the limits of 78°K and 800°K.

(b) A bare tungsten tip is first cooled to

* Both Mignolet and Hermann used films for their measurements.

** Minus signs of Miller indices are omitted throughout this paper, as they have no absolute physical meaning.

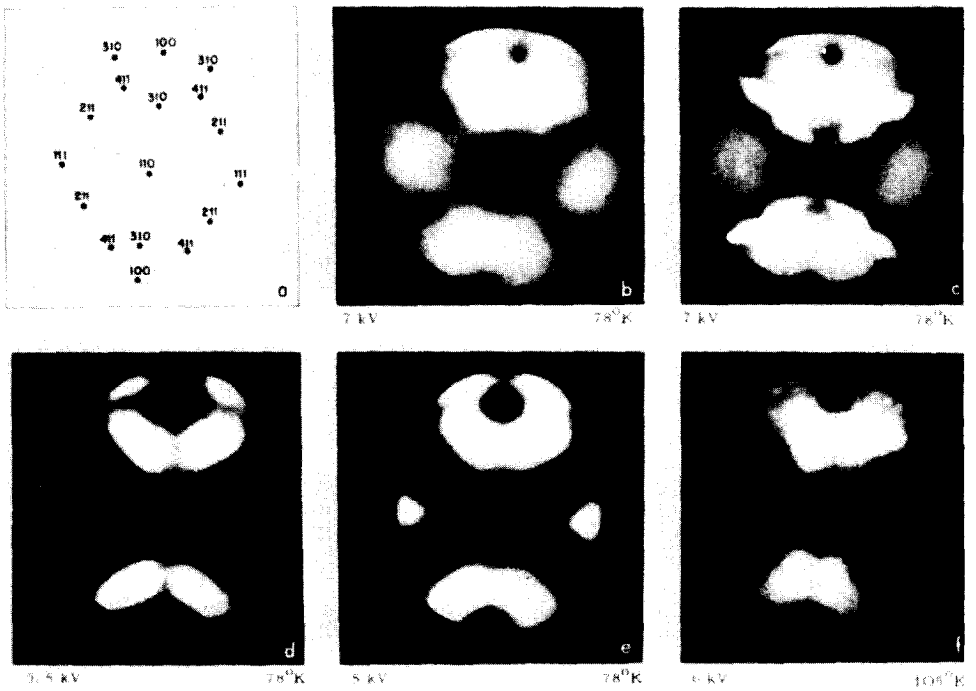

FIG. 1. Adsorption of xenon on tungsten. a. Polar projection of crystal lattice. b.–f. Successively obtained emission patterns. Accelerating voltages and temperatures are given below each photograph.

78°K under high vacuum and then exposed to hydrogen. Subsequently the temperature is changed as in experiments of type (a).

(c) After a certain adsorption state is established, hydrogen is pumped off and the tip temperature is decreased.

Fig. 2 shows plots of work function versus temperature for the three sets of experiments.

The emission patterns for several characteristic adsorption states are shown in Fig. 3 and 4.

From Fig. 2 it is seen that the curves *sub* (a) are almost reversible, although a small hysteresis separates the branches of ascending and descending temperatures. The curve (b) is distinctly different from (a) in the low-temperature range; but once the tip has been warmed up, curve (b) further follows the path of (a). Obviously the distribution of hydrogen over the surface is then in equilibrium. Surface diffusion, necessary to establish equilibrium, appears to be blocked below a temperature of ~160°K. The onset of surface diffusion at 160°K had also been observed by Gomer (*14*).

These conclusions are illustrated by a comparison of the emission patterns in Fig. 3 and 4. In case (a) (Fig. 3b) the pattern is neatly "crystalline" showing the "frozen

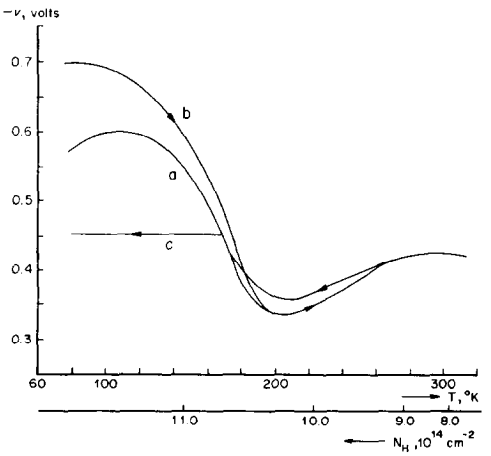

FIG. 2. Surface potential of hydrogen on tungsten vs. temperature and coverage.

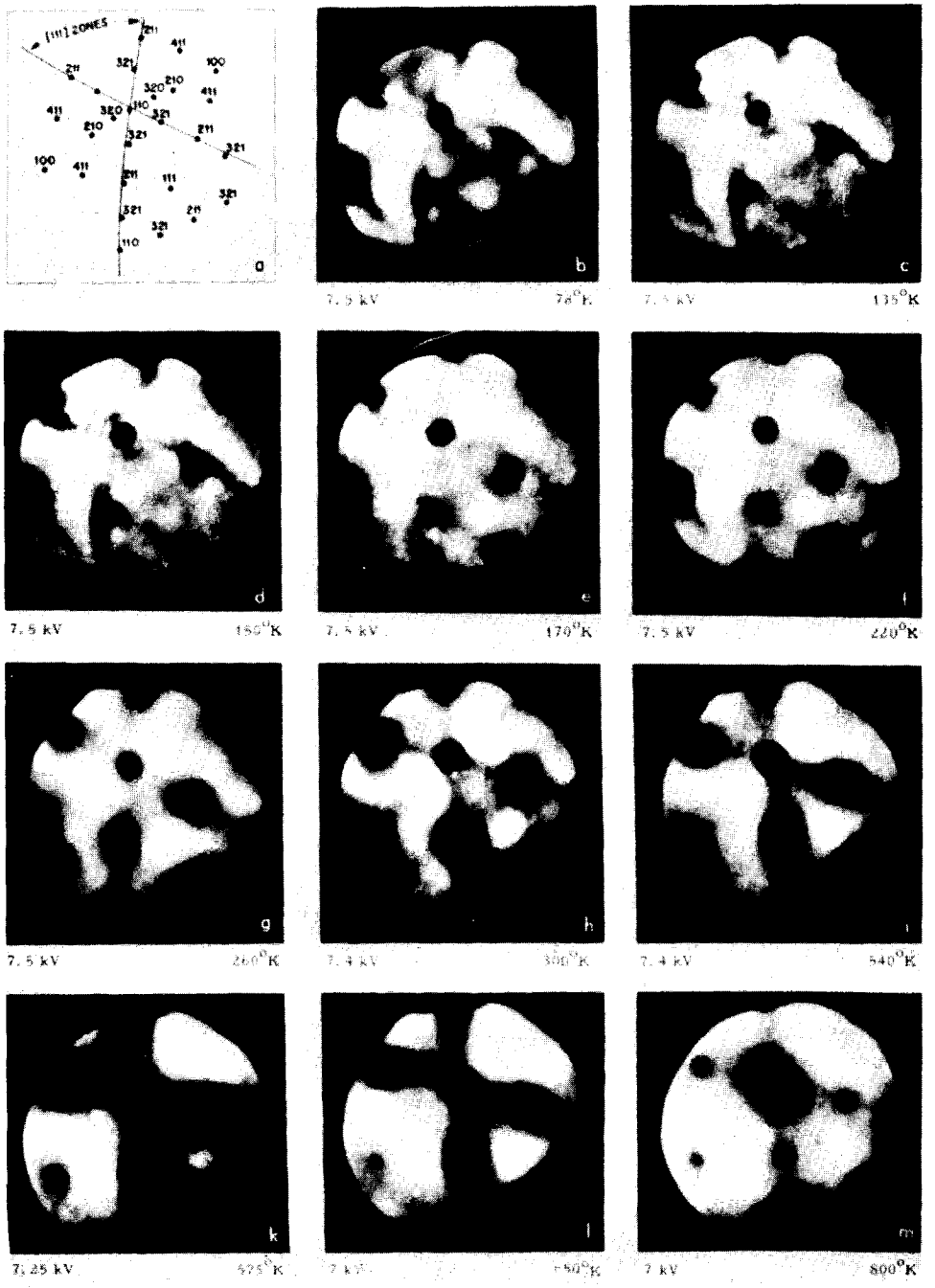

FIG. 3. Desorption of hydrogen from tungsten, case (a).

in" equilibrium of the adsorbate, immobilized at 160°K. In case (b) (Fig. 4b) the pattern is much more uniform; the distribution is caused by the sticking coefficients controlling the alighting of molecules, which hit the surface at random. Obviously the sticking coefficients depend only little on the crystalline nature of the surface. Once the temperature is brought above the critical limit of 160°K, hydrogen will

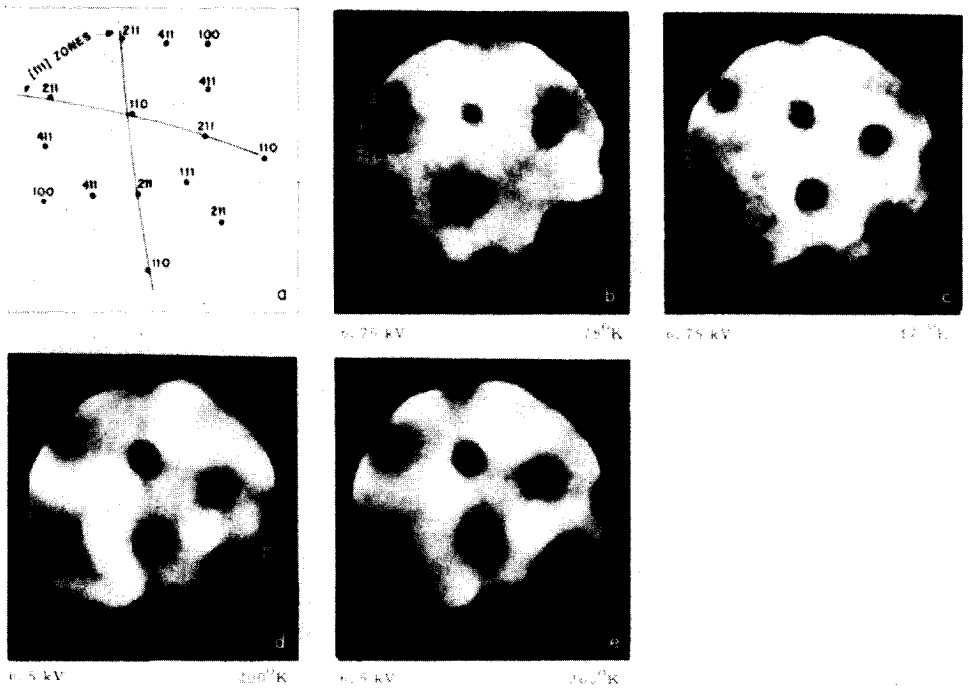

FIG. 4. Desorption of hydrogen from tungsten, case (b).

migrate and equilibrium will be established; cases (a) and (b) then become indistinguishable.

In case (c) emission pattern and work function are found to remain unchanged, when the temperature drops in the absence of hydrogen. This shows that the results found in experiment (a) are due to additional adsorptions from the gas phase and not to some temperature dependence of bonding states, or to mere diffusions of the adsorbate over the surface. In other words, it is justified to interpret the results obtained in experiments (a) and (b) in terms of changing coverage, although, in fact, T was varied. The results of the present isobaric method are therefore comparable to data obtained by varying the coverage isothermally, e.g. by steady admission of gas to a film. The coverage N_H, expressed in hydrogen atoms/cm^2 of the tungsten surface, can be calculated from the temperature and pressure, since the function N_H (p,T) is known from Hickmott's data (*9*). In Fig. 2 the resulting N_H scale is shown below the T scale. It should, however, be remembered, that Hickmott's data were measured on macroscopic wires, the surfaces of which differ in crystalline composition from hemispherical tips. The N_H scale, therefore, is not intended to provide more than a rough orientation. For unravelling this complex adsorption system further, the results of (a) are most relevant. The fate of the hydrogen-covered surface when heated from 78°K to 800°K can be summarized as follows:

(1) The complete adsorption layer at 78°K has an over-all surface potential of −0.57 volt. The emission pattern shows bright areas at the (411), (320), and (111) faces and along the [111] zone, with the exception of the (211) face.
(2) On heating to 130°K, an increase in work function results, indicating a desorption of "positive" hydrogen. The decrease in emission is most pronounced at the faces (111), (411), and (320). The same desorption can be partly achieved by pumping at 78°K.
(3) Between 150°K and 200°K "negative"

hydrogen is desorbed and the work function is markedly decreased on most faces. The remnants of the original bright bands along the [111] zones disappear.

(4) At 220°K the work function slightly increases. Desorption of a positive adsorbate takes place, predominantly from the (411) faces and along the [111] zones.

(5) The remaining negative hydrogen is gradually removed by further heating. The heat of adsorption of this stable adsorbate is different for different faces and increases in the order

$$(111) < (320) < (411) < (100) < (211)$$

The (211) faces are denuded by heating for 100 sec at 760°K, which corresponds to a heat of adsorption of

$$\Delta H_{(211)} = 46 \text{ kcal/mole}$$

The reverse sequence of emission patterns is found during adsorption at e.g. 300°K. It seems therefore safe to conclude that the reversibility of the surface potentials, which is shown in Fig. 2 for the total surface, also holds for each individual surface element.

Phenomenologically, the three extrema of curve (a) indicate four hydrogen complexes of distinguishable polarities. This, admittedly, is an arbitrary definition, dictated by the particular method of investigation. In a previous article (*17*) it was shown that different methods of investigation yield different numbers of distinguishable complexes. The four complexes can be characterized as follows:

Complex A. Strongly bound H atoms with negative surface potential ($v = -0.43$ volt), desorbing above 280°K. The heat of adsorption is 20–46 kcal/mole, depending on the crystal plane. Complex A is most strongly held on (211) faces.

Complex B. Positively polarized, desorbing between 220° and 280°K. Its heat of adsorption varies between 15 and 20 kcal/mole. This state is preferentially observed on (411) faces and their environment.

Complex C. Negatively polarized, desorbing at 120°–200°K. The heat of adsorption is in the range of 8–14 kcal/mole. It is preferentially adsorbed on (411) and neighboring faces.

Complex D. Weakly bound, positively polarized state. The heat of adsorption is in the range of 6–10 kcal/mole. Mainly found on (411), (111), and (320) faces and along the [111] zone.

C. Other Chemisorption Systems

a. Hydrogen on Platinum

Figure 5 shows the surface potential as a function of temperature. In agreement with Mignolet's results (*18*), two hydrogen species are discerned, a negative type of high heat of adsorption and a positive, less stable, adsorbate. The work function, when plotted versus the temperature, consequently passes through a maximum. From the p, T, θ relationship, established by Schuit and Van Reyen (*19*) for the adsorption on Pt/SiO_2, the coverage θ can be calculated. For the maximum we find $\theta \approx 0.4$, which corresponds well with the location of the maximum in Mignolet's data.

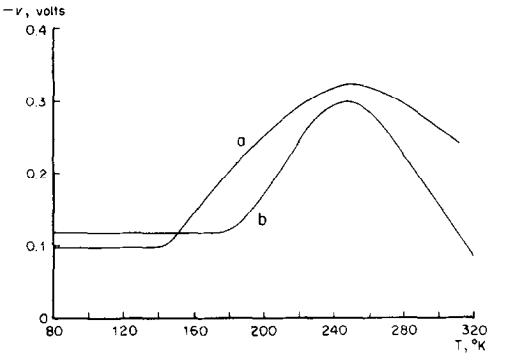

FIG. 5. Surface potential of hydrogen on platinum during desorption; a, $p_{H_2} = 4 \times 10^{-6}$ mm Hg; b, $p_{H_2} = 10^{-9}$ mm Hg.

In contrast to what is observed in the adsorption of hydrogen on tungsten, the field-emission pattern of a hydrogen-covered tip is very similar to that of a clean tip and little surface heterogeneity is detected for the two hydrogen complexes on

TABLE 1
ADSORPTION STATES OF CO ON W

	State		ΔH (kcal/mole)		N_{CO} (10^{14} cm^{-2})	Charge on CO	Location on surface
Author[a]	E	R	E	RRS	E	RRS	RRS
	α	29	20	20	1	Positive	All faces
	β_1	57	—	52	—	Negative	(411)(310)(210) faces
	β_2	69	75	70	4.5	Negative	(111) and other faces
	β_3	74–77	100	100	—	Negative	[111] zone

[a] E = Ehrlich, R = Redhead, RRS = present authors.

platinum. Only a ring around (110) appears to have an enhanced affinity for hydrogen; for this ring a heat of adsorption of 26 kcal/mole is found.

b. Carbon Monoxide on Tungsten

Four adsorption states are discerned. They can easily be correlated with the four species, distinguished by Ehrlich (*8*)

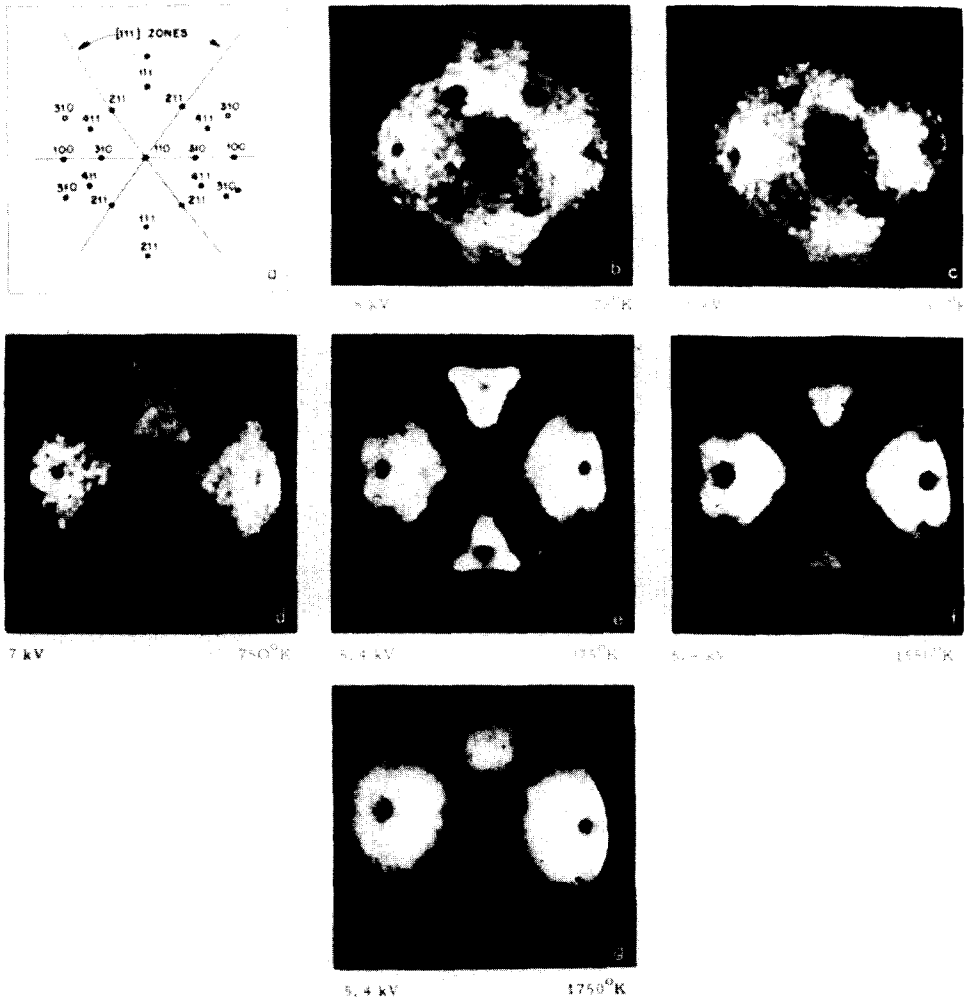

FIG. 6. Desorption of CO from tungsten after adsorption at 700°K and subsequent cooling under CO.

and by Redhead (*20*) by means of the flash filament technique, as can be seen from Table 1. From the field emission patterns shown in Fig. 6 it is clear that β_1, β_2, and β_3 refer to adsorptions at different faces, whereas the α-state is more or less uniformly distributed as was previously found by Klein (*21*). The work function maximum corresponds to $v = -0.92$ volt. A value of -0.84 volt was measured by Klein (*21*) by the same method, whereas Eisinger (*22*) reports a value of -0.94 volt from photoelectric measurements on the (311) face of a tungsten ribbon. The α-state has a positive charge, reducing the surface potential to -0.72 volt, which might suggest adsorption on top of the preadsorbed CO layer, as was assumed by Culver, Pritchard, and Tompkins (*23*).

c. CO on Platinum

Only one state is detected; the negative surface potential does not pass through a minimum. This result is in agreement with earlier findings by Eischens *et al.* (*24*) and by Dorgelo and Sachtler (*25*). The surface potential at high coverage is -0.68 volt; the heat of adsorption at low coverage amounts to 32 kcal/mole.

d. Formic Acid on Tungsten and on Platinum

We have previously published field-emission studies of HCOOH on tungsten (*26*). The adsorption proper is followed by a rearrangement of the metal atoms in the surface, called "surface corrosion."

On platinum no surface corrosion can occur, since the rate of decomposition of the adsorbate on platinum is higher than the mobility of the surface atoms. At 300°K the adsorption complex exhibits a negative surface potential of -1.55 volts. This value shows that on platinum the adsorbate is more negative than adsorbed hydrogen (-0.33 volt, see Fig. 5); carbon monoxide (-0.68 volt, see above) and even oxygen [-1.1 volts (*27*)]. The adsorbate is, therefore, fairly properly described as a formate anion. This conclusion had previously been drawn (*28, 29*) from the infrared spectrum of the adsorbate on e.g. nickel; but with that method some authors (*30*) had obtained data which were at variance with ours. The present data seem to decide the controversy in favor of the formate anion.

Decomposition of this formate which is detected even at room temperature causes

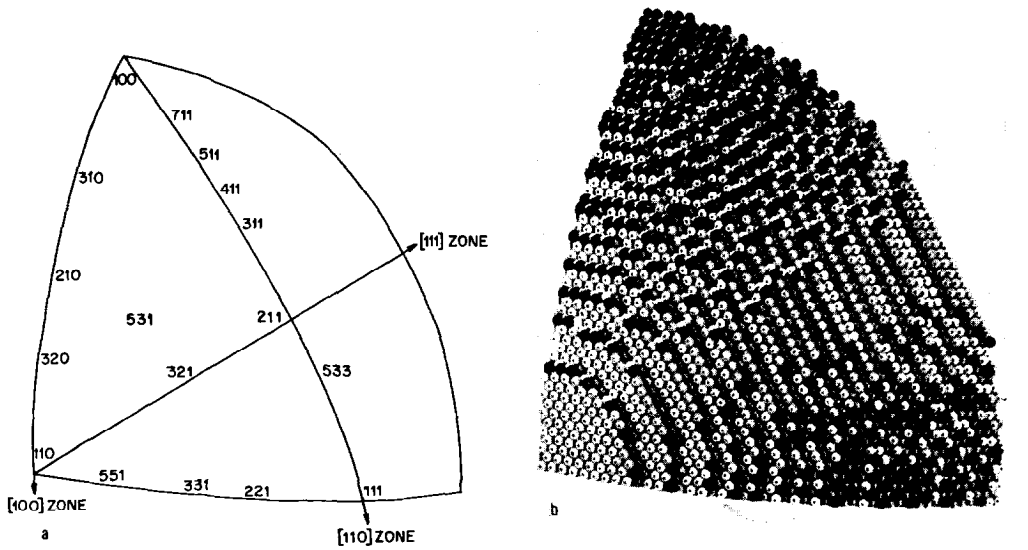

FIG. 7. Atomic arrangement at the spherical surface of a body-centered cubic crystal. (a) Polar projection. (b) Model. Shades represent various degrees of unsaturation.

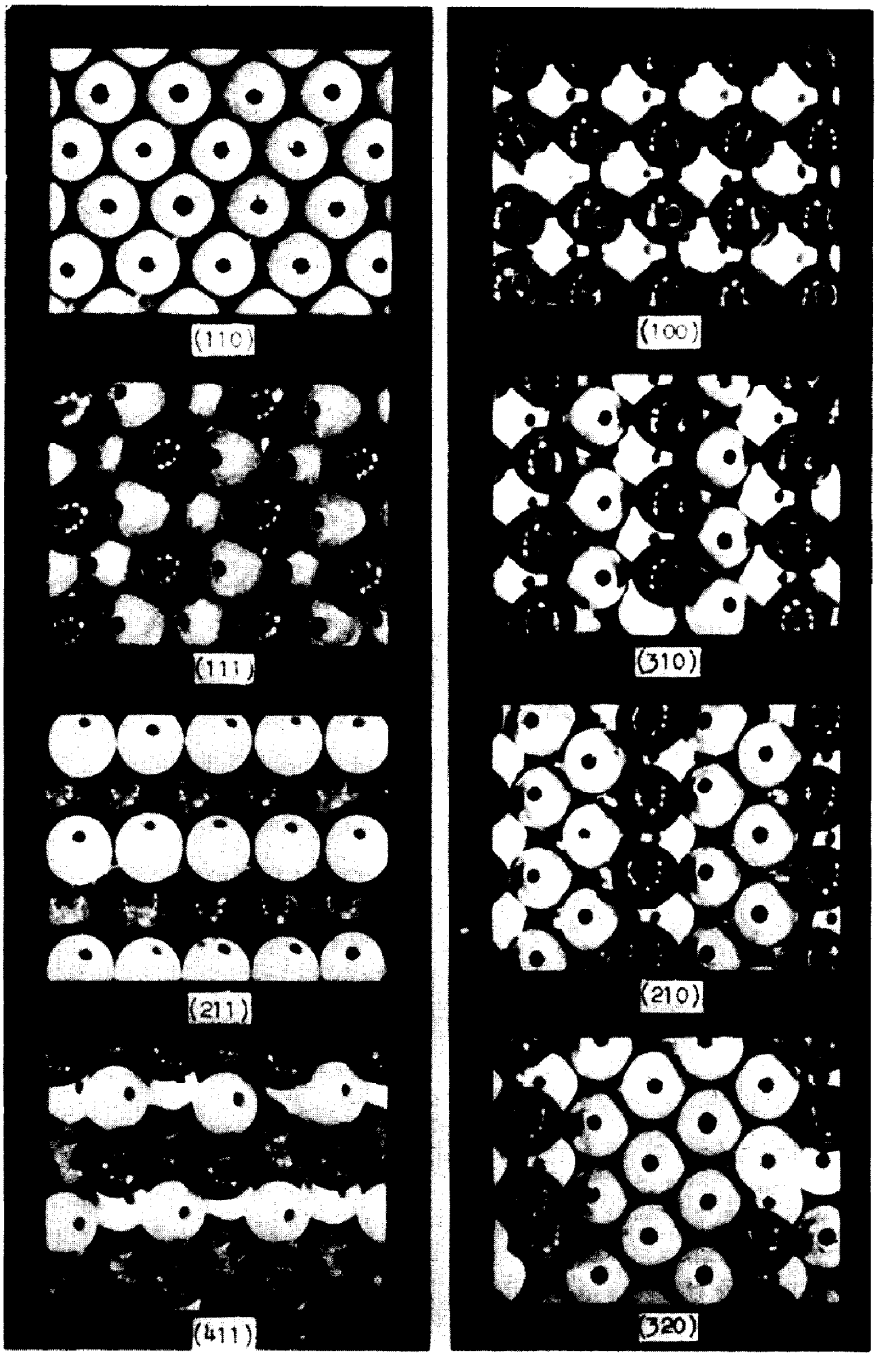

FIG. 8. Atomic arrangement in various faces of b.c.c. lattice.

a decrease in work function. The rate of this decrease is consistent with the rate data given by Sachtler and Fahrenfort (*28*) for the decomposition of superficial formates (0.01 molec·site^{-1}·sec^{-1} for Pt at 300°K).

IV. Discussion

A. Surface Topography

In discussing the properties of individual adsorption sites, one can take advantage of the close analogy which exists between

chemisorption and the growth of a metal crystal in its own vapor (*12, 31*). Different areas on the surface of a hemispherical crystal can be distinguished according to the

1. topographic atom configurations
2. different degrees of unsaturation.

The atomic configurations are illustrated by models, of which Fig. 7, 8, and 9 show reproductions.

The degree of unsaturation (of the individual surface atoms) is conveniently expressed by the number of missing first neighbors. A tungsten atom in the interior of a tungsten crystal, for example, has 8 first neighbors, a tungsten atom in a (110) face on the surface has only 6 neighbors, its degree of unsaturation, expressed in this convenient terminology, is therefore $n = 8 - 6 = 2$. In Table 2 the concentrations of various sorts of unsaturated atoms are shown for the important crystal faces of the b.c.c. and f.c.c. lattices. As in the b.c.c. lattice the distance to the second-closest neighbors is only 15% greater than the distance between closest neighbors, the unsaturation with respect to second neighbors has also been included in the table for this lattice.

There is a close relation between the atomic configuration of an adsorption site and its degree of unsaturation. Let us suppose that on a given site the adsorbate can simultaneously contact m surface atoms, from each of which n neighbors are missing in comparison with full coordination. A simple consideration then shows that for the condition of crystal growth

$$n = m$$

If the site is different from the sites used in crystal growth, however, or if the size of the adsorbate differs strongly from the size of a metal atom, this simple relation no longer holds. Instead, the tendency to seek sites of high unsaturation will then compete with the tendency to achieve high ligancy for the adsorbate. For a number of cases the present results allow comparison of the relative importance of these two driving forces.

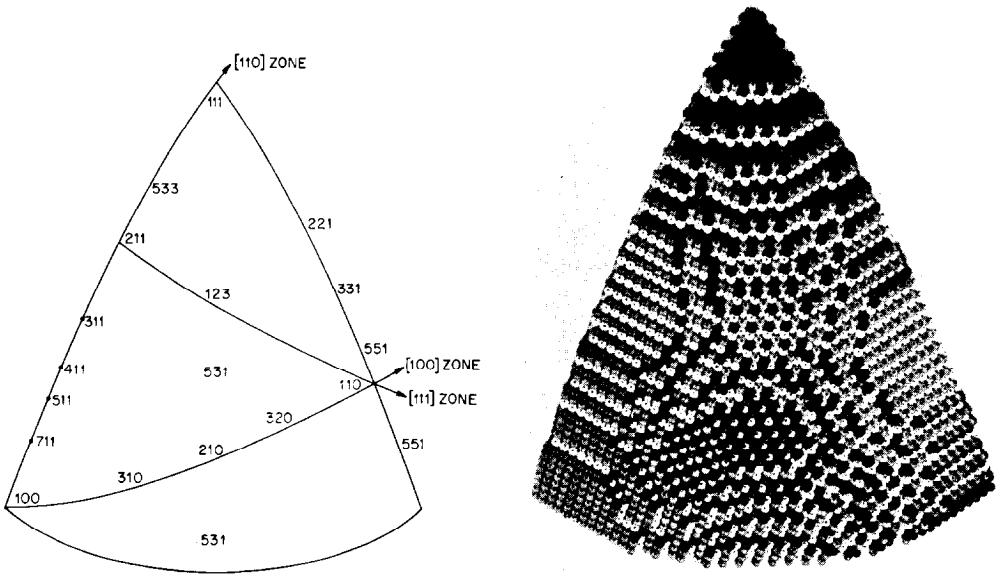

FIG. 9. Atomic arrangement at the spherical surface of a face-centered cubic crystal.

B. Physical Adsorption

The studies on the adsorption of xenon on tungsten by Ehrlich *et al.* (*6*) and those reported in the present article show that physical adsorption at low coverage displays a very pronounced topographical sensitivity. Similarly Roberts (*32*) had

observed that physical adsorption below monolayer coverage depnds on the nature of the adsorbing surface, e.g. on the presence of a chemisorbed layer.

If the atomic configurations of the adsorbing sites are considered, it is easy to understand why the heat of adsorption is highest for the (411) faces. These faces are characterized by widely spaced W_4 atoms (the subscript indicates the number of missing first neighbors), protruding from the surface. Between these W_4 atoms, bowl-shaped adsorption sites are formed. The van der Waals radius of xenon is such that it perfectly fits in such a bowl. The xenon atom then is in simultaneous contact with three W_4 atoms, two W_3 atoms and one W_1 atom. An analysis of the geometry shows that the contact with all six neighbors may be considered perfect, all distances agreeing with the ideal distances to within one-half per cent. It is difficult to escape the conclusion that this ideal surrounding is the reason why the xenon prefers these "tailor-made" adsorption sites, although the absolute concentration of W_4 atoms in the (411) face is not exceptionally high.

When all these bowl-shaped sites in the (411) plane are filled, a surface area per adsorbed atom of 21 Å^2 results, which is markedly different from the value of 17.2 Å^2 derived from the density of liquid xenon and often used in BET determinations of surface areas.

The (111) faces also offer protruding unsaturated metal atoms, but the geometrical arrangement is much less favorable for adsorbing xenon, and consequently a smaller heat of adsorption is found. No bowls of appropriate size are found on smooth faces such as (100) on which indeed no xenon adsorption is observed at the pressures and temperatures studied by us. Since these faces are characterized by a very high concentration of W_4 atoms, the results suggest that for the physical adsorption of xenon the principle of maximum ligancy is much more important than the unsaturation of the surface atoms.

From the measured heats it follows that at low coverage at 78°K the equilibrium distribution over the (411) and the (111) faces should be

$$\frac{\theta_{(411)}}{\theta_{(111)}} = \exp\left(\frac{7500 - 5000}{78R}\right) \sim 10^7$$

As this equilibrium distribution is established by migration of adsorbed xenon over the surface, the (411) faces are mainly populated from their borders. The atoms arriving first are precipitated near the border, and a sharp diffusion front moves

TABLE 2

CONCENTRATIONS OF ATOMS OF VARIOUS DEGREES OF UNSATURATION ON SOME CRYSTAL FACES OF F.C.C. AND B.C.C. LATTICES[a]

	f.c.c.[b]					b.c.c.[b]			
$(hkl)/n$	6-	5-	4-	3-	2-	4-	3-	2-	1-
100	—	—	13.0	—	—	10.0 (1)	—	—	—
310	4.1	—	4.1	4.1	—	6.3 (2)	—	6.3 (2)	—
210	5.8	—	—	5.8	—	4.5 (2)	—	8.9 (2)	—
320	3.6	3.6	—	3.6	3.6	2.8 (2)	—	11.2 (2)	—
110	—	9.2	—	—	9.2	—	—	14.1 (2)	—
211	—	5.3	—	5.3	5.3	—	8.2 (3)	—	8.2 (1)
411	—	6.2	3.1	—	6.1	4.7 (3)	4.7 (1)	—	4.7 (1)
511	—	4.8	4.8	—	4.8	—	—	—	—
111	—	—	—	16.0	—	5.8 (3)	—	—	5.75 (3) 5.75 (1)
Tip average	2.5	5	2.5	3	2	4.5	3	4.5	2

[a] All concentrations expressed in 10^{14} cm^{-2}; n = number of missing first neighbors. The numbers between brackets indicate the missing second-nearest neighbors for the b.c.c. lattice.

[b] Numerical values based on lattice parameters of Pt and W, respectively.

towards the center of each (411) face. This boundary diffusion causes the sharp bright arcs, expanding from the border of the (411) faces to their interior.

C. Chemisorption

The emission patterns of platinum and tungsten after chemisorption show that topographic heterogeneity is more pronounced on the rough surface of b.c.c. crystals than on the rather smooth f.c.c. crystals. When various adsorbates are compared, hydrogen, small enough to detect even slight differences in atomic arrangements, shows an exceptionally high topographic sensitivity. We shall, therefore, essentially limit our discussion of the chemisorbed systems to this particularly instructive example. The most stable hydrogen complex A can be correlated with the concentration of W_4 and W_3 atoms. This complex is identified with the well-known and often investigated "normal" dissociative chemisorption of hydrogen; each H atom is linked to the surface by a predominantly covalent bond. As the present results show, this bond is tightest on those crystal faces where the unsaturated W atoms are grouped in protruding rows, e.g. on the (211) face and other planes of the [111] zone. From data measured by Becker (*11*) it is derived that at room temperature and a hydrogen pressure of 10^{-8} mm Hg the surface potentials on individual faces are proportional—within each zone—to the sum of the numbers of the W_3 and W_4 atoms. Evidently, only weak chemisorption can occur on the (110) faces since these consist solely of W_2 atoms.

The most stable complex of CO on tungsten shows a configurational preference similar to that of hydrogen complex A. Again, the faces of the [111] zones, such as (211), exhibit the highest heat of adsorption, although these faces are not highest in degree of unsaturation. Obviously, the arrangement of W_3 atoms in protruding rows, which easily allows any small adsorbate to come into simultaneous contact with two unsaturated surface atoms, is attractive for both H and CO.

The two hydrogen complexes B and C are characterized by a preference for the (411) faces and their environment. The tungsten atoms in these faces are very widely spaced; the actual nonplanar surface is, consequently, composed of a considerable number of successive lattice planes. It is plausible that a great variety of adsorbing sites will result, and it seems natural that these regions should be the only parts of the total surface which are capable of accomodating four different hydrogen complexes simultaneously.

The weakest hydrogen complex D may consist of H_2 units, but it certainly is not a physisorbate. By definition, physical adsorption is confined to temperatures near the boiling point of the adsorbate, and this type of sorption was indeed detected by Beeck, Givens, and Ritchie (*33*) for hydrogen on metal films at temperatures below the range of our present experiments. Moreover, the heat of adsorption of complex D is roughly equal to the heat of adsorption of xenon, whereas the polarizability of hydrogen is much smaller than that of xenon; consequently, a pure van der Waals-London type of adsorption is not consistent with the properties of complex D. Even the weak, positive hydrogen complex D is most strongly held on the rows of W_3 atoms in the faces of the [111] zone. From most faces this complex is desorbed at 130°K, but from the [111] zone only between 150 and 200°K.

In view of the conclusion that hydrogen and CO generally prefer sites of two adjacent unsaturated W atoms, it is surprising that the (411) faces should bind these adsorbates less strongly than the faces of the [111] zones. A possible explanation might be the fact that the W_3 atoms in the (411) faces are more highly coordinated with second neighbors than the W_3 atoms in the [111] zones.

The adsorption types defined as A and D are identical with the negative and positive adsorptions of hydrogen on tungsten, studied extensively by Mignolet (*34*) and Hickmott (*9*). They used tungsten films (contact potential technique) or macroscopic wires (flash filament technique) as adsorbants. It is not so difficult to understand why complexes B and C have not

been detected by these techniques. In Fig. 10 a qualitative plot of the individual work functions of three crystallographic zones is given for the conditions of curve (a) in Fig. 2. The individual work functions are estimated from the measured over-all work function and the relative

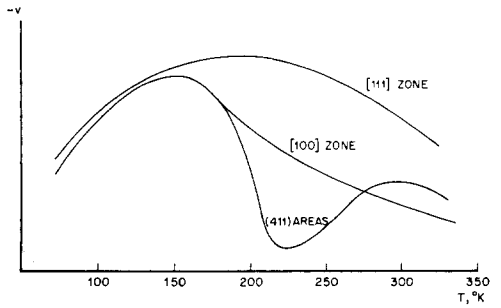

FIG. 10. Surface potential of hydrogen on different faces of tungsten.

brightnesses of the faces in the emission patterns. As the complexes B and C, which flank the pronounced minimum, occur exclusively in the (411) region, they can only be detected by a technique which registers even these relatively small and unstable surface elements. Since in field emission the areas of low work function contribute greatly to the over-all electron emission, this technique is particularly suited to the investigation of unstable surface elements. The situation is completely different in contact potential measurements, where the surface elements are weighed according to their geometric area, which gives little chance to small facets. Moreover, the films which were used in Mignolet's (*34*) work may have differed somewhat in their crystallographic surface compositions from the tungsten tips used in the present work.* On macroscopic wires, finally, the unstable faces will be absent altogether, because—in thermodynamic equilibrium—their occurrence in the total crystal surface decreases with increasing crystal size.

The present results are at variance with Becker's (*11*). That author observed work function changes $\Delta\Phi$ on a given crystal face (hkl) while hydrogen was slowly admitted at room temperature. He assumed that the adsorbate concentration θ was equal on all crystal faces and, consequently, he attributed breaks in the measured $\Delta\Phi$ versus θ plots to successively formed hydrogen complexes of different dipole moments. The present results, on the contrary, imply that only *one* hydrogen complex is present on the surface at room temperature, its polarity being more or less the same on all crystal faces. But since the heats of adsorption for this complex are different on different faces, the adsorbate concentrations on different surface elements θ_{hkl} will differ by orders of magnitude at low over-all coverage. Hence, different faces are populated successively. When a given face "gets its turn" and becomes covered, this will, necessarily, result in a steep rise of the local work function, causing a marked break in the observed $\Delta\Phi$ vs. θ plot.

V. CONCLUSIONS

The results enable us to give the following answers to the questions brought up in the introduction.

1. Ample evidence has been found for the existence on a tungsten surface of a very pronounced *a priori* heterogeneity, attributable to the topographic nature of the adsorbing surfaces. The heats of adsorption for negative and for positive hydrogen and for the β-complexes of CO, but also for physisorbed xenon show very pronounced differences when different faces are compared. The resulting equilibrium distribution of any of these adsorbates over the total surface is nonuniform; at low coverage the adsorbate is concentrated on a few crystal faces. The preference of xenon for certain adsorption sites can easily be understood by considering the purely geometrical principle of maximum ligancy only. In the case of chemisorption, both this

* The crystallographic nature of the surface of evaporated films can be estimated from work function measurements. For a tungsten film with a surface composition identical to that of the tips, the work function should be 4.50 volts. For a film surface consisting exclusively of the most stable (110) faces, a work function of 5.9 volts would result (*35*). The value which is actually measured, viz. 4.6 volts for slightly sintered films (*36*), shows that faces with high Miller indices also participate in the surface of tungsten films.

geometrical factor and the chemical unsaturation of the surface atoms seem to determine the attractiveness of a site.

The role of the topographic *a priori* heterogeneity is also illustrated by the fact that only those crystal faces which display a great variety of adsorption sites are able to accommodate four different hydrogen complexes simultaneously.

2. The results do not exclude, however, the concept of an "induced" heterogeneity. It even seems likely that induced effects must be invoked to explain e.g. the strong decrease of heats of adsorption with increasing coverage on f.c.c. metals which, as the present results show, exhibit only little *a priori* heterogeneity. Moreover, a positive and a negative hydrogen complex are found on all crystal faces of platinum and of tungsten. It is impossible to decide whether the presence of the stable negative complex A is a necessary prerequisite for the subsequent positive adsorption of D, or whether different types of sites should be considered even within each adsorbing plane, as was suggested previously (*12*, *37*).

Acknowledgments

Our thanks are due to Mr. A. M. van den Broeck and Mr. G. J. H. Dorgelo for their skilful help with the experiments.

References

1. Suhrmann, R., *Physik. Z.* **30,** 939 (1929); *Z. Elektrochem.* **35,** 68 (1929).
2. Mignolet, J. C. P., *Discussions Faraday Soc.* **8,** 105 (1950).
3. Sachtler, W. M. H., and Dorgelo, G. J. H., *Bull. Soc. Chim. Belges* **67,** 465 (1958).
4. Suhrmann, R., Mizushima, Y., Hermann, A., and Wedler, G., *Z. physik. Chem.* (*Frankfurt*) **20,** 332–52 (1959).
5. Ponec, V., Knor, Z., *in* "Actes du 2ième Congrès Intern. de la Catalyse," p. 195. Editions Technip, Paris, 1961.
6. Ehrlich, G., Hudda, F. G., *J. Chem. Phys.* **30,** 493 (1959).
7. Ehrlich, G., *J. Chem. Phys.* **34,** 29 (1961).
8. Ehrlich, G., *J. Chem. Phys.* **34,** 39 (1961).
9. Hickmott, T. W., *J. Chem. Phys.* **32,** 810 (1960).
10. Becker, J. A., *Advances in Catalysis* **7,** 135 (1955).
11. Becker, J. A., *in* "Actes du 2ième Congrès International de la Catalyse," p. 1777. Editions Technip, Paris, 1961.
12. Sachtler, W. M. H., Dorgelo, G. J. H., *in* "Proc. 4th Intern. Conference on Electron Microscopy," p. 51. Springer, Berlin, 1960.
13. Good, R. H., Jr., Müller, E. W., *in* "Handbuch der Physik" (S. F. Flügge, ed.), Vol. 21, p. 176. Springer, Berlin, 1956.
14. Gomer, R., "Field Emission and Field Ionization." Harvard University Press, Cambridge, 1961.
15. Mignolet, J. C. P., *Rec. Trav. Chim.* **74,** 685 (1955).
16. Hermann, H., "Lichtelektrische Untersuchungen über die elektronische Wechselwirkung zwischen adsorbierten Xenonatomen und aufgedampften Wolfram- und Nickelschichten." Thesis, Braunschweig, Germany, 1955.
17. Sachtler, W. M. H., and van Reijen, L. L., *Shokubai* (*Tokyo*) **4,** 147 (1962).
18. Mignolet, J. C. P., *J. Chim. Phys.* **54,** 19 (1957).
19. Schuit, G. C. A., and van Reijen, L. L., *Advances in Catalysis* **10,** 242 (1958).
20. Redhead, P., *Trans. Faraday Soc.* **57,** 461 (1961).
21. Klein, R., *J. Chem. Phys.* **31,** 1306 (1959).
22. Eisinger, J., *J. Chem. Phys.* **27,** 1206 (1957).
23. Culver, R., Pritchard, J., and Tompkins, F. C., *Z. Elektrochem* **63,** 741 (1959).
24. Eischens, R. P., Francis, S. A., and Pliskin, W. A., *J. Phys. Chem.* **60,** 194 (1956).
25. Dorgelo, G. J. H., and Sachtler, W. M. H., *Naturwissenschaften* **46,** 576 (1959).
26. Rootsaert, W. J. M., and Sachtler, W. M. H., *Z. physik. Chem.* (*Frankfurt*) **26,** 16 (1960).
27. Giner, J., and Lange, E., *Naturwissenschaften* **40,** 506 (1953).
28. Sachtler, W. M. H., and Fahrenfort, J., *in* "Actes du 2ième Congrès International de la Catalyse," p. 831. Editions Technip, Paris, 1961.
29. Hirota, K., Kuwata, K., Otaki, T., and Asai, Sh., *ibid.*, p. 809.
30. Eischens, R. P., and Pliskin, W. A., *ibid.*, p. 789.
31. Stranski, I. N., and Suhrmann, R., *Ann. Physik* (6.F.) **1,** 169 (1947).
32. Roberts, M. Wyn, *Trans. Faraday Soc.* **56,** 128 (1960).
33. Beeck, O., Givens, J. W., and Ritchie, A. W., *J. Colloid Sci.* **5,** 141 (1950).
34. Mignolet, J. C. P., *J. Chem. Phys.* **20,** 341 (1952); *Rec. trav. chim.* **74,** 685 (1959).
35. Young, R. D., and Müller, E. W., *J. appl. Phys.* **33,** 91 (1962).

36. SUHRMANN, R., AND WEDLER, G., *Z. angew. Phys.* **14,** 70 (1962).

37. MIGNOLET, J. C. P., "Etude Théorique et Expérimentale de Quelques Problèmes d'Adsorption," Memoires de la Société Royale des Sciences de Liège, 5ième série, Tome **1,** fasc. 3 (1958).